

**VERMICULITE MINERALIZATION ASSOCIATED WITH ULTRAMAFICS
IN AGASTHYAPURA AREA, MYSORE DIST., KARNATAKA STATE,
INDIA - A MINERALOGICAL STUDY**

**Kikkeri N. PRAKASH NARASIMHA^{1)*}, Honnaiah RAMALINGAIAH¹⁾, Karel MELKA²⁾,
K. KRISHNAVENI¹⁾, Pinnelli S. R. PRASAD³⁾, Chikkamadaiah KRISHNAIAH⁴⁾,
Katihalli S. JAYAPPA⁴⁾ and Atni V. GANESHA⁴⁾**

¹⁾ *Department of Geology, University of Mysore, Manasagangotri, Mysore-570 006, India*

²⁾ *Institute of Geology, Academy of Sciences of the Czech Republic, Rozvojová 135, 165 02, Praha 6-Lysolaje, Czech Republic*

³⁾ *P.S. R. Prasad, M.P.D, N.G.R.I, Hyderabad-500 007, India*

⁴⁾ *Ocean Science and Technology Cell (Marine Geology and Geophysics), Mangalore University, Mangalagangotri, Mangalore- 574199, India*

**Corresponding author's e-mail: prakashnarasimha@yahoo.com*

(Received September 2006, accepted November 2006)

ABSTRACT

Vermiculite in its macroscopic form occurs in the Archaean supracrustal rocks exposed towards east of Sargur supracrustal complex in Karnataka state. The present study forms the first detailed work on the occurrence of vermiculite associated with the ultramafic rocks in the Agasthyapura, which lies in the long. 76° 50' 658" and lat. 12° 15' 976". Petrography, X-ray diffraction, FTIR, DTA&TGA, SEM, fluid inclusion and electron probe analyses are presented in this contribution study. The probable origin of vermiculite from biotite through hydrobiotite is discussed.

KEYWORDS: vermiculite, hydrobiotite, Sargurs, Agasthyapura, Mysore district, Karnataka

1. INTRODUCTION

Vermiculite, the name which is derived from the Latin word *vermiculare*, to breed worms, is a platy mineral much similar to mica with a composition of hydrated silicate mineral with the general formula: $(\text{Mg,Ca})_{0.33} (\text{Mg, Fe, Al})_3 (\text{Si, Al})_4 \text{O}_{10} (\text{OH})_2 \cdot 4\text{H}_2\text{O}$. When heated, the vermiculite plates expand at right angles to the cleavage (accordion-like) as the contained water is converted to steam. These elongated, worm like, light-weight particles can expand from 6 to as much as 30 times to their original volume in the long dimension. In its natural state the mineral has little useful application. Thus vermiculite finds a variety of applications in industry (electrical, concrete, fertilizer, etc.) only after exfoliation.

Vermiculite occurrences have been described from several parts of the world, such as Pavagada in Karnataka state, India (Radhakrishna, 1948); Gopalpura in Karnataka state (Prakash Narasimha et al., 2004, 2006); the Palamau district, Bihar, India (Chattopadhyay and Bhattacharya, 1994); Nagasaki Prefecture, Japan (Nakamura, 1981); in the Malaguide Complex, Spain (Ruiz Cruz, 2003; Ruiz Cruz and Novak, 2003); near Hafafit, Egypt (El Shazly et al., 1975); Central Turkey (Fatma Toksoy-Koksal et al., 2001) and in several areas of the United States (Bassett, 1959; Bush, 1976; Van Gosen et al., 2002).

Mostly vermiculites form by alteration of micas. The major elemental composition of vermiculites is closely related to that of the parent mica, although there is partial disruption of the mica structure (Jelitto et al., 1993). Vermiculite resulting from the alteration of micas commonly involves the replacement of the interlayer K by a hydrated cation, generally Mg (Moore and Reynolds, 1989; Nemezc, 1981; Fatma Toksoy-Koksal et al., 2001).

Macroscopic vermiculite formation was attributed to either hydrothermal (Morel, 1955) and/or supergene processes (de la Calle and Suquet, 1988; Zhelyaskova-Panayotova et al., 1992, 1993; Fatma Toksoy-Koksal et al., 2001). As to experimental studies (Roy and Romo, 1957; Komarneni and Roy, 1981) vermiculite is a product of mica alteration by dilute low-alkali solutions.

Vermiculite in its macroscopic form occurs in the supracrustal rocks of 3400-3100 Ma old, exposed towards east of Sargur complex in Karnataka state (Fig. 1). The present study forms the first detailed work on the occurrence of vermiculite associated with the ultramafic rocks in the Agasthyapura, which lies in the long. 76° 50' 658" and lat. 12° 15' 976". In this paper for the first time the report on the origin of the vermiculite formation of Agasthyapura is discussed. Agasthyapura area falls east of the Sargur supracrustal

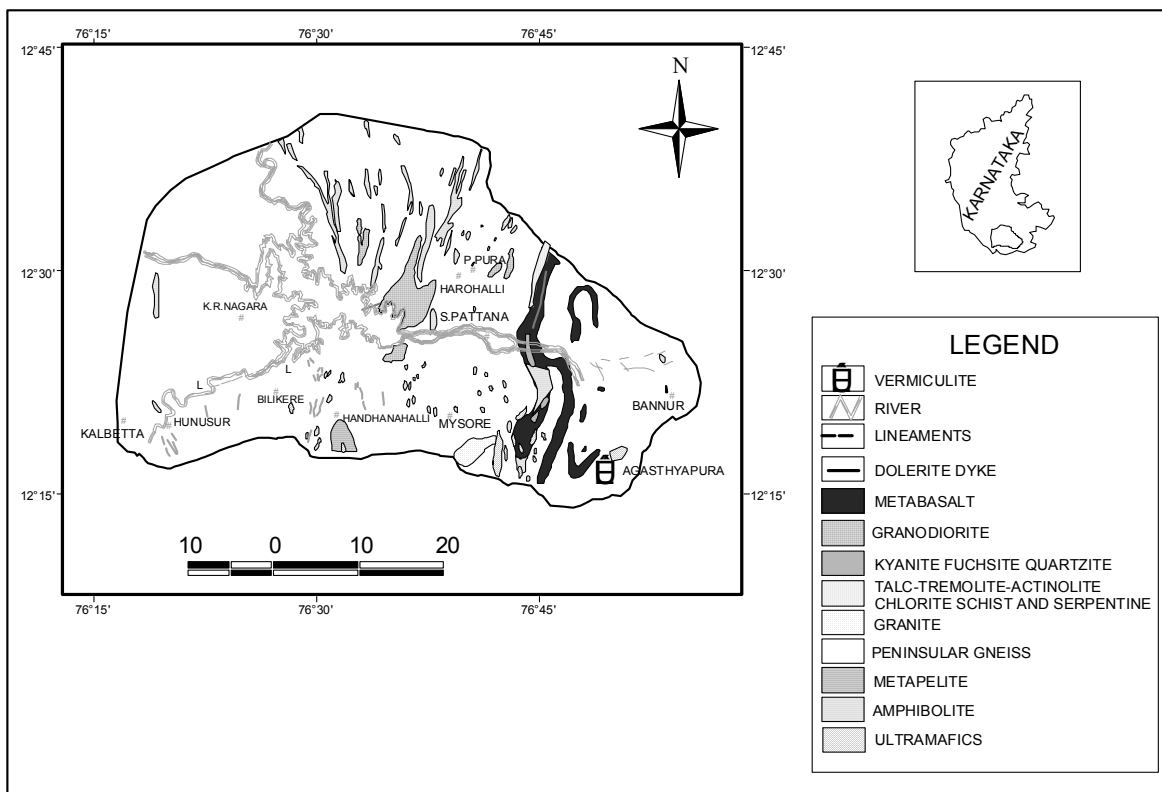


Fig. 1 Simplified geological map of the Sargur schist complex showing vermiculite occurrence of Agasthyapura area.

complex, which forms a zone of high-grade metamorphic assemblages scattered within a migmatite gneissic complex (Fig. 1). They are mainly composed of diverse igneous and sedimentary lithologies, such as ultramafic-mafic intrusive bodies, pelites, quartzites, impure carbonates, iron formations and enclaves of anorthosites. The ultramafic bodies occur as enclaves within the gneissic complex, obscuring the original relationship. The contact of the supracrustals with the gneissic complex is generally concordant and marked by intense migmatization (Swaminath and Ramakrishna, 1981; Radhakrishna and Vaidyanadhan, 1997). The ultramafic litho-units are cut by late acidic (felsic) intrusions.

Vermiculite mineralization in the Agasthyapura area occurs within the ultramafic body which trends in N35°E direction and at the contact zones between the N65°E trending and dipping subvertical acid (felsic) intrusive rocks. The vermiculite accumulations occur as clots within the ultramafic body and also as narrow belts, found in the marginal portions of fractured and altered ultramafic rocks in contact with acid intrusive (Fig. 2).

Veins of vermiculite are parallel to the trend of the acid intrusive rocks and the vermiculite formation decreases as the depth increases. Within the mineralized zone hornblendites show well developed

crystals of hornblende and trend in N45°E direction, which shows alteration to vermiculite. The ultramafic body, where the mineralization is noticed, is around 100 m in length and it has a variable width, which ranges from 2m to as much as 15m. Ultramafic rock is traversed by joints trending in different directions such as N30°, N170° and N110°.

2. PETROGRAPHY

Petrographic observations have been made for the different litho-units of the Agasthyapura deposit such as ultramafic rock, acid intrusives and hornblendites.

Microscopic studies of the host ultramafic rocks found that they are mainly made up of clinopyroxene + carbonate + opaques. Clinopyroxenes show different degrees of alteration, mainly altering to biotite, actinolite and chlorite. Clinopyroxenes are subhedral non-pleochroic grains with well-developed cleavages, show alteration to colourless and non-pleochroic actinolite grains. Carbonate veins traverse them. Exsolved phases of opaques are noticed along the cleavages and grain boundaries of the clinopyroxene grains. Clinopyroxenes show pronounced alteration to biotite and chlorite. Vermiculite is brownish black in hand specimen and is brownish yellow in thin section and non-pleochroic with

inclined extinction. Vermiculites are always found as rims around the grains of clinopyroxene (Fig. 3) and are also interwoven with biotite grains indicating their alteration from biotite through an intermediate stage - hydrobiotite.

Biotite in this study refers to a regular 1:1 interstratified (mixed-layer) biotite-vermiculite, a mineral recognized in many vermiculite deposits (Boettcher, 1966). Petrographic observations indicate that growth of vermiculite observed in the ultramafic samples occurred after the formation of biotite through an intermediate stage of hydrobiotite, in agreement with studies of vermiculite deposits elsewhere (Prasad and Majumdar, 1966; Nettleton et al., 1973; Tarzi and Protz, 1979; Ghabru et al., 1987).

The acid intrusion is in the form of quartz veins. They include bigger grains of quartz surrounded with smaller grains (recrystallized) in variable proportions. Bigger quartz grains are fractured with characteristic undulose extinction. Hornblende shows equigranular texture and consists mainly of green coloured subhedral hornblende grains. They are pleochroic from light green to yellowish green. Hornblende grains are highly fractured and these fractures are filled with vermiculite material, which traverses across the grains and along grain boundaries. Hornblendes show alteration to vermiculite in the form of rims (Fig. 4).

3. X-RAY DIFFRACTION

The X-ray diffraction analyses were carried out using Philips automatic apparatus X'Pert APD with the graphite monochromator. A region from 2θ $\text{CuK}\alpha$ 2° to 75° of the pattern was run by using scanning speed $1^\circ/\text{min}$. X-ray beam was demarcated by $\frac{1}{2}^\circ$ divergence slit, 0.1mm receiving slit and $\frac{1}{2}^\circ$ scatter slit. Electric conditions on the X-ray tube were as follows: 40kV/40mA. The analyses were carried out on the separated crystal flakes, which were mounted directly on the glass slide with a trace of adhesive. The material was not ground. By this way basal diffractions of crystal flakes were enhanced in the recorded pattern. This manner of preparation was advantageous for the identification.

Fig. 5a represents the XRD pattern of the Agasthyapura vermiculite sample. Vermiculite is identified by its basal reflections: 14.23 Å (002), 7.16 Å (004), 4.78 Å (006), 3.60 Å (008), 2.88 Å (00,10), 2.39 Å (00,12), 2.05 Å (00,14), 1.79 Å (00,16), 1.59 Å (00,18), 1.43 Å (00,20), 1.30 Å (00,22). This X-ray pattern is distinctive of vermiculite with its very intensive ~ 14 Å diffraction. The following 7 Å line has a small intensity. Afterwards higher orders basal diffractions increase their intensities till the fifth one.

Fig. 5b represents the XRD pattern of hydrobiotite (a specific mineral name for mixed-layer structure with regularly alternating biotite and vermiculite components). Its identification was performed on the basis of the following basal diffractions: 23.5 Å (001), 11.8 Å (002), 8.6 Å (003),

6.25 Å (004), 4.95 Å (005), 4.10 Å (006), 3.45 Å (007), 3.09 Å (008), 2.73 Å (009), 2.48 Å (00,10), 2.04 Å (00,12), 1.90 Å (00,13), 1.66 Å (00,15), 1.56 Å (00,16), 1.44 Å (00,18).

Hydrobiotite has the mixed layer structure formed of regularly alternating biotite and vermiculite sheets in the proportion 1:1. In case of regular interstratification such structures have a privilege of using their own mineral names- in our case hydrobiotite. It is characterized by high value of its basal diffraction (our sample has $d_{001} \sim 23.5$ Å), higher orders of which can be derived after dividing by whole numbers. Layers A (biotite) and B (vermiculite) are combined according to the following scheme: ABABABAB. It means that A (biotite) sheet is surrounded with B (vermiculite) sheet from each side (Melka, 2000; Melka et al., 2000; Melka, 2005).

On the basis of fifteen 00ℓ diffractions up to 18th order, mean d_{001} for hydrobiotite was calculated. The value $24.70 \text{ Å} \pm 0.65$ was received for the diffraction pattern in Fig. 5b.

4. THERMAL ANALYSES

The pulverized samples were used for thermal analyses. They were continuously heated at the heating rate of $10^\circ \text{C}/\text{min}$. DTA and TG analyses were carried out. In both of them platinum crucibles were taken.

In case of differential thermal analyses (DTA) Al_2O_3 was used as a comparable sample. Thermogravimetric analyses (TG) were performed on the TG-750 device of the firm Stanton Redcroft. In case of DTA the initial weight of the sample was 50mg, for TG analysis ~ 10.4 mg were used.

Fig. 6a represents the DTA and TG curves of the pure vermiculite from the studied area. Doubled endothermic effect on DTA curve in the low-temperature region registers the moisture and the release of molecular water from the interlayer positions of vermiculite. Another small endothermic effect takes place at 550°C . Endothermic peak at $\sim 850^\circ \text{C}$ can be interpreted as the escape of hydroxyl water from octahedral positions of the vermiculite structure, which is destroyed at this temperature. Following exothermic peak indicates the crystallization of enstatite. Thermogravimetric curve registers 17.5 % loss in mass at 900°C .

Together with DTA also thermogravimetric curve (TG) is drawn in a single diagram for hydrobiotite in Fig. 6b. Differential thermal analysis exhibits very intensive endothermic peak which has three minima (at $\sim 90^\circ \text{C}$, 110°C and near to 200°C). They document the release of molecular water from the examined sample. DTA curve has the similar appearance like the curve of vermiculite. This component forms a part of the hydrobiotite crystal structure and is responsible for its behaviour during heating. TG curve exhibits ~ 7 % loss in mass at 900°C . It is less than in case of vermiculite. A main difference between hydrobiotite and vermiculite from

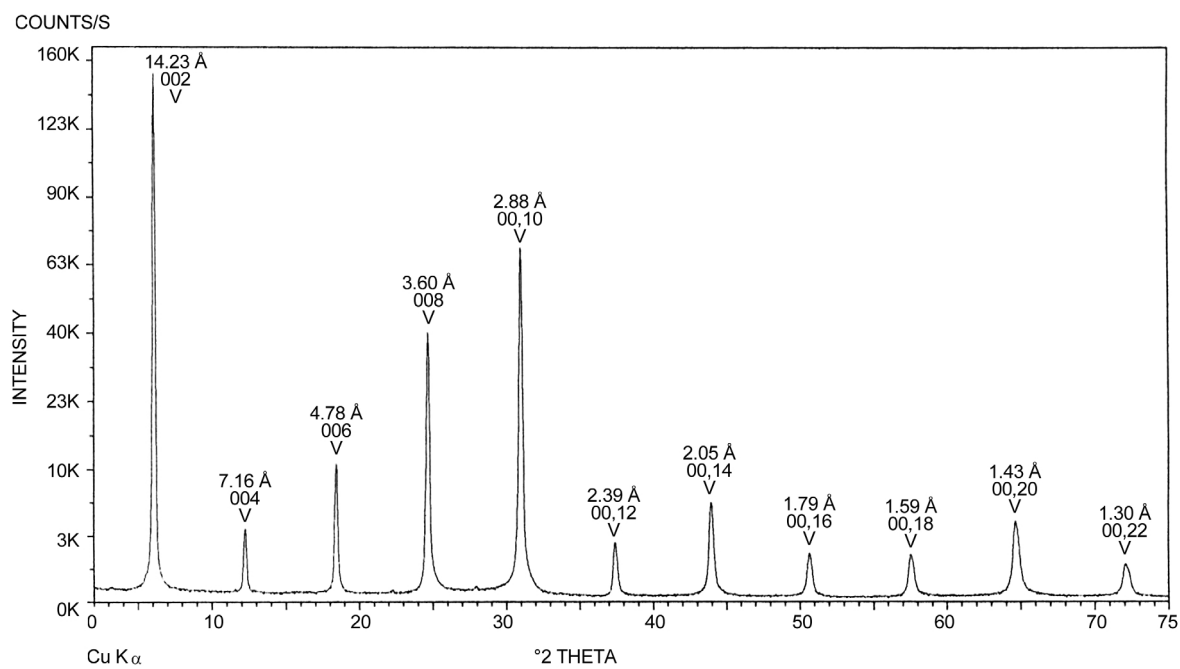


Fig. 5a XRD pattern of the raw vermiculite.

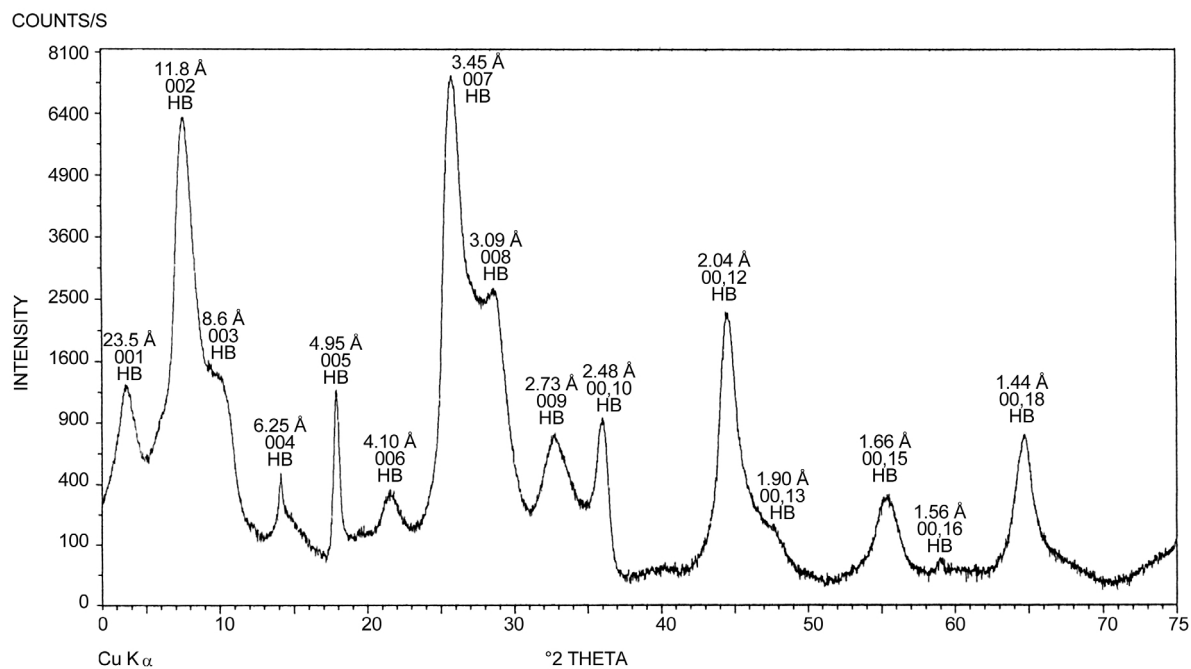


Fig. 5b XRD pattern of hydrobiotite.

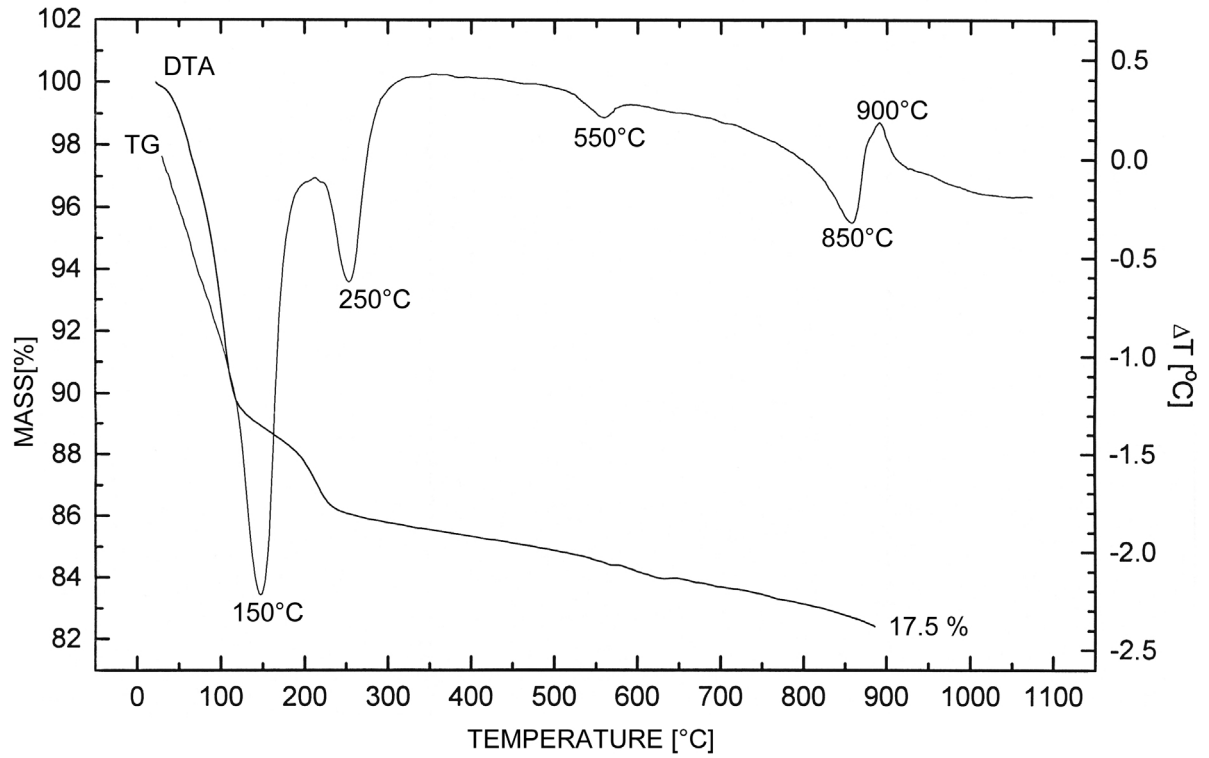


Fig. 6a DTA and TG curves of the pure Agasthyapura vermiculite.

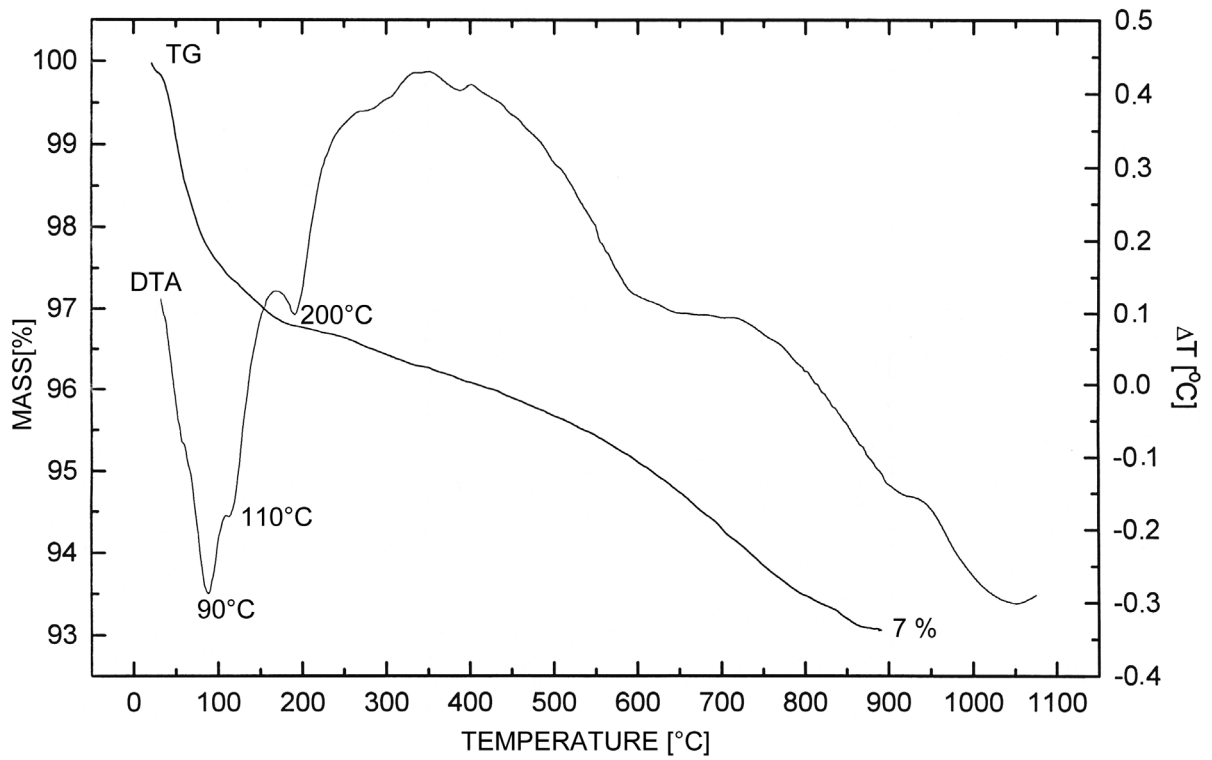


Fig. 6b DTA and TG curves of hydrobiotite from Agasthyapura.

Table 1 Mineral chemistry of representative hydrobiotite and vermiculite grains, Agasthyapura.

HYDROBIOTITE				VERMICULITE			
SiO ₂	38.7	38.1	38.9	38.8	39.4	39.1	40.2
TiO ₂	1.38	1.28	1.36	0.54	0.57	39.1	0.59
Al ₂ O ₃	15.1	15.0	15.2	13.9	14.5	14.2	14.6
FeO	8.61	9.65	8.50	8.22	7.77	8.61	8.35
MnO	0.03	0.02	0.04	0.08	0.07	0.06	0.06
MgO	21.4	20.8	21.0	21.8	22.4	22.4	22.7
CaO	0.20	0.20	0.20	0.63	0.61	0.69	0.87
Na ₂ O	0.11	0.15	0.17	0.00	0.00	0.00	0.02
K ₂ O	2.53	2.25	2.36	0.06	0.01	0.05	0.03
F	0.49	0.36	0.29	0.67	0.67	0.52	0.77
Cl	0.00	0.01	0.0	0.03	0.02	0.03	0.03
Total	88.55	87.82	88.02	84.46	85.62	82.83	84.96
CATIONS							
Si	5.740	5.714	5.784	5.877	5.857	5.844	5.901
Ti	0.151	0.145	0.153	0.061	0.064	0.062	0.071
Al	2.666	2.649	2.660	2.474	2.538	2.507	2.451
Fe	1.069	1.210	1.058	1.041	0.966	1.075	0.987
Mn	0.00	0.004	0.005	0.011	0.009	0.007	0.012
Mg	4.605	4.654	4.656	4.926	4.960	4.984	4.886
Ca	0.035	0.032	0.049	0.102	0.098	0.111	0.122
Na	0.051	0.045	0.049	0.00	0.00	0.001	0.004
K	0.480	0.430	0.447	0.011	0.003	0.00	0.005
F	0.229	0.170	0.138	0.322	0.314	0.247	0.363
Cl	0.000	0.000	0.001	0.000	0.000	0.000	0.000
Total	15.02	14.99	15.23	14.82	14.80	14.93	14.83

the chemical point of view is in the amount of potassium and water. Hydrobiotite contains less water contrary to vermiculite. Only little potassium is present in vermiculite. Comparing to biotite its amount is lowered in hydrobiotite.

5. ELECTRON MICROPROBE ANALYSIS

Electron probe microanalysis was performed using a JEOL 8900 Microprobe equipped with wavelength dispersive spectroscopy. A total of 21 analyses were made on each sample, measuring 3 spots from 7 different grains within each sample. Selected analytical results are shown in Table 1.

Analyses of hydrobiotite grains found SiO₂ values of 38.1 to 38.9 wt. %, MgO values ranging from 20.8 to 21.3 wt. % (as the amount of Mg is prevailing over Fe, the chemical composition is closer to phlogopite than to biotite) and CaO values varying from 0.20 to 0.22 wt. %. The hydrobiotite grains contain higher percentages of K (1.20 to 2.53 wt. % K₂O). SiO₂ values in the vermiculite grains vary from 38.8 to 40.2 wt. %. These vermiculites show only subtle differences in CaO and MgO content compared to hydrobiotites. A distinct contrast in K₂O content exists between vermiculite and hydrobiotite grains (only 0.01 to 0.06 K₂O wt. % in the vermiculite). This suggests that the Agasthyapura vermiculites have

undergone nearly complete transformation from mica to vermiculite.

6. FLUID INCLUSION STUDIES

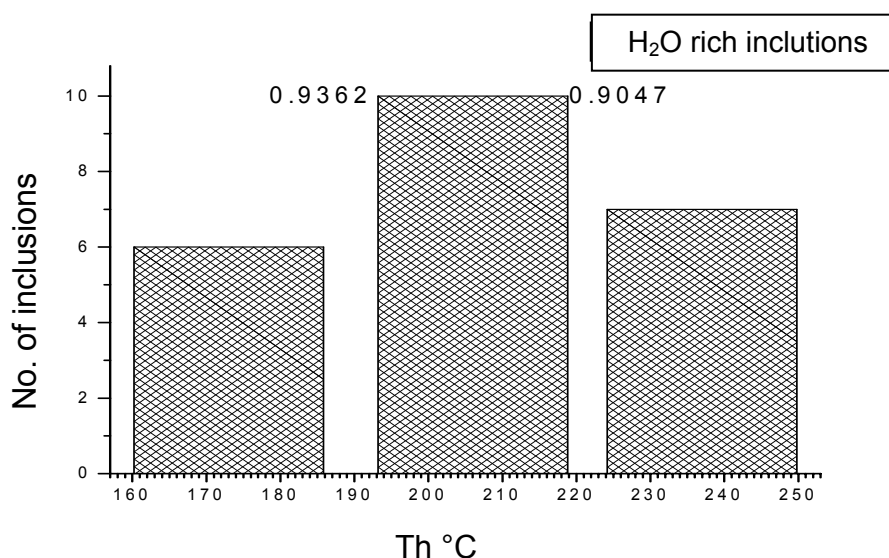
Based on the preliminary optical studies, sample of acid intrusive was selected for a detailed study of the fluid-inclusion species. Phase transitions of fluid inclusions were made on a temperature calibrated LINKAM heating and freezing apparatus (with a range of -180 to 600 °C). Microthermometric results are presented in Table 2. The salinity values for aqueous inclusions have been calculated after the method of Sourirajan and Kennedy (1962) and the density data after Lemlein and Klevstov (1961).

Acid intrusive associated with the vermiculite formation is mainly in the form of quartz vein. The quartz grains host the fluid inclusion species, which are oval to rounded in shape. The inclusions are biphasic at room temperature and range in size from less than a micron to almost 10 microns. These inclusions are randomly distributed within the quartz grain (Fig. 7a).

Heating and freezing experiments were carried out on biphasic inclusions present in quartz grains. They show initial melting temperature of -12.1 °C suggesting that the biphasic inclusions are saline aqueous inclusions and the melting temperature yields

Table 2 Microthermometric results.

Sl.no	Samples no.	Rock name	Mineral	T _m °C	H ₂ O rich inclusions		
					Wt % NaCl equiv.	Th °C	d g/cc
1	AP2	Acid intrusive	Quartz	-12.1	16	173	0.959
						206.4	0.928
						237	0.889

**Fig. 7b** Histogram plot of the H₂O-rich inclusions.

salinity value of 16 wt % NaCl equiv. (Sourirajan and Kennedy, 1962). Homogenization of biphasic aqueous inclusions into liquid phase varies between temperatures of 173 °C to 237 °C with a mean peak between 193 °C and 219 °C (Fig. 7b) corresponding to the density values of 0.936 g cm⁻³ and 0.904 g cm⁻³ (Lemlein and Klevstov, 1961).

7. INFRARED SPECTROSCOPY STUDIES

Fourier transfer infrared spectroscopy (FTIR) studies were carried out with a NEXUS FTIR spectrometer from Thermo-Nicolet, using a thermoelectrically cooled deuterated triglycine sulphate (DTGS) detector, extended range KBr (XT-KBr) beam splitter, and a dual source, capable of working in the wavenumber range 375 – 12500 cm⁻¹. The sample, a thin plate of about 20 µm thick, was placed on an aperture of about one mm. The spectra reported in this study are recorded using the wavenumber region 1500 to 10000 with a white light source (tungsten halogen); each spectrum is the average of 256 scans using a resolution of 2 cm⁻¹. The conventional KBr pellet method has also been followed to record the network silicate modes and to check the repeatability of the

data. The spectra in the wavenumber range 400 to 4000 cm⁻¹, using NEXUS Ever-Glo source, are the resultant of 256 scans. Typical uncertainties in the peak positions are ~2 cm⁻¹ for the sharper and stronger modes, while that for the weak and overlapping modes could be ~5 cm⁻¹.

The FTIR spectra of vermiculites closely resemble those of biotite and phlogopite. However, certain differences in the OH stretching band region are prominent (Fig. 8a). As shown in Figure 8a, the fundamental OH stretching region due to water molecules (held in the vermiculite layers) occurs around 3400 cm⁻¹ (ν_{OH}) and the corresponding bending vibration is clearly observed at 1632 cm⁻¹ (δ_{OH}). The shoulder peak at around 3572 cm⁻¹ indicates the presence of OH groups coordinated with other cations. More detailed information about atomic arrangement around OH groups is delineated in the combination modes involving OH stretch and Al-OH bending modes in the wave number region 4000 – 8000 cm⁻¹. Spectral features observed in these vermiculites are broadly comparable to those reported earlier by Cariati et al. (1983). The combination modes due to ($\nu_{OH} + 2\delta_{OH}$) are observed around

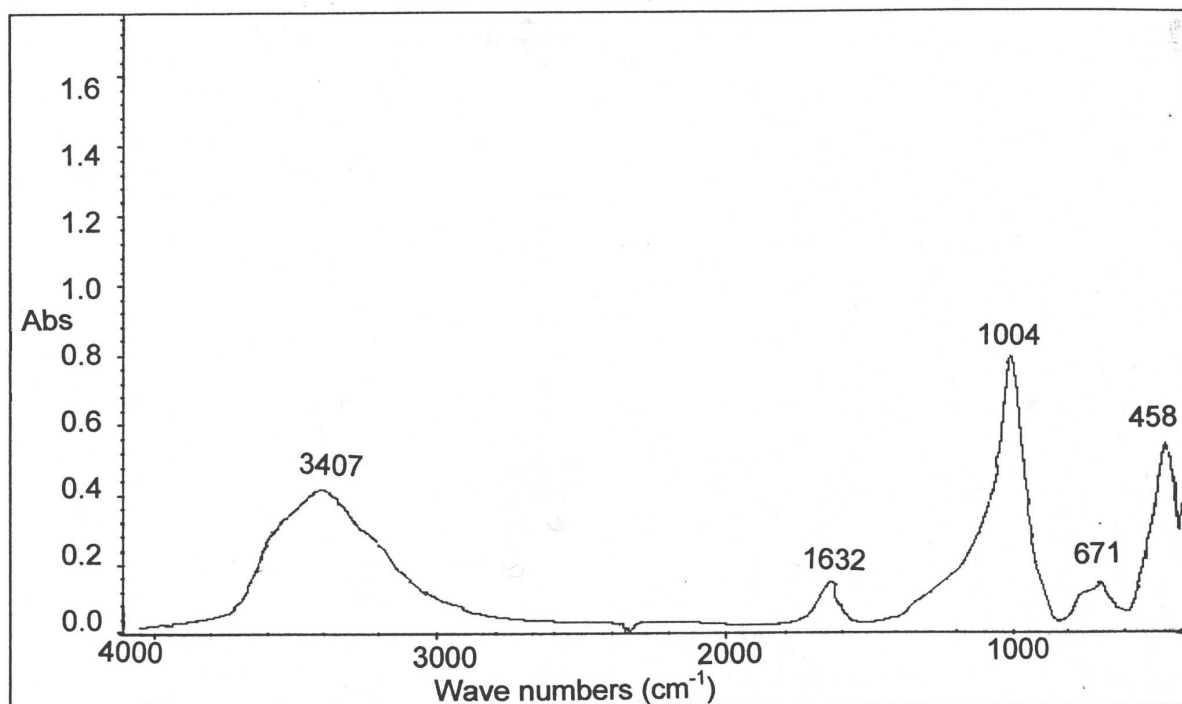


Fig. 8a Background corrected FTIR spectra of vermiculites recorded in KBr pellets.

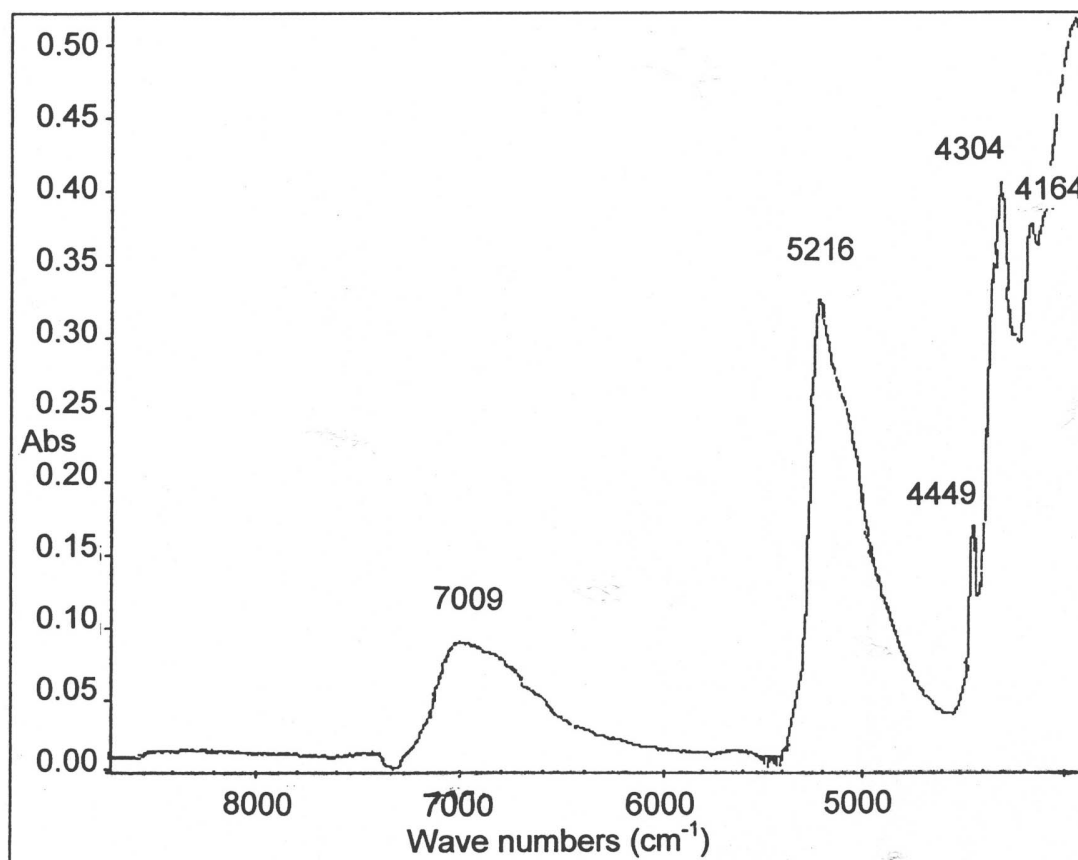
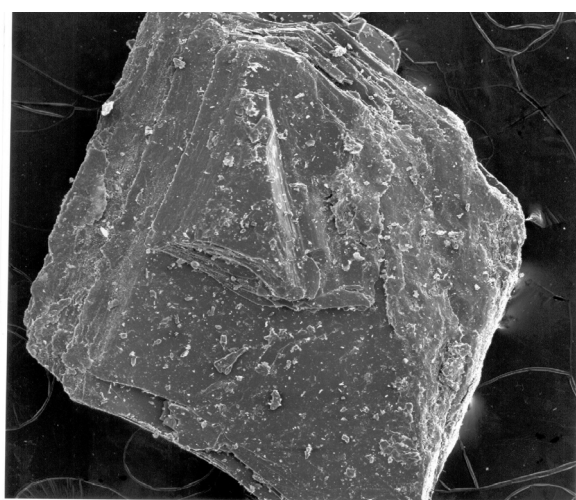


Fig. 8b Background corrected FTIR spectra of vermiculite wafers of about 20 μm thick, in the wavenumber region 4000 – 8000 cm⁻¹.

Table 3 Semi-quantitative EDS analyses of vermiculites.

ELEMENT	%	IONS
Na	0.45	0.16
Mg	14.08	4.64
Al	0.01	0.00
Si	27.37	7.81
K	0.06	0.01
Ca	0.44	0.09
Ti	0.16	0.03
Cr	0.01	0.00
Mn	0.54	0.08
Fe	12.03	1.73
O	45.89	23

**Figs. 9a and 9b** SEM photographs of the raw and exfoliated vermiculites.

6990 cm^{-1} . The asymmetry of this band is attributed to variations in the strength of hydrogen bonding schemes of water molecules (Fig. 8b). Similar band structure is found for the mode due to $(\nu_{\text{OH}} + \delta_{\text{OH}})$, which has been observed around 5210 cm^{-1} . Corresponding modes reported by Cariati et al. (1983) for vermiculites from Libby, Montana, occur at 7052 cm^{-1} (1418 nm) and 5202 cm^{-1} (1922 nm), respectively.

8. SCANNING ELECTRON MICROSCOPE (SEM)

Splits of the samples were analyzed by X-ray diffraction (XRD) and examined visually using JEOL 5800-LV scanning electron microscope (SEM), equipped with an Oxford ISIS energy-dispersive X-ray spectrometer (EDS). The EDS provides semi-quantitative analyses of individual mineral particles and stoichiometric calculations. EDS analyses were conducted on single, isolated mineral particles.

* = 22 Sigma

Sample- Si Sample location-Agasthyapura

Sample No-AP-V

Particle No- AP-V-1

Particle description- FeMg amphibole

Other minerals identified: Vermiculite, Hornblende, Fe-Oxides

SEM of the platy morphology raw vermiculite sample shows superimposed flakes with individual layers very closely spaced. Exfoliated vermiculite flakes, created by heating the sample, indicate accordion like expansion and the expansion is one and halftimes the raw sample (Figs. 9a and 9b). Individual expanded layer measures <0.1 cm to as much as 1 cm. EDS analyses indicated semi-quantitatively the presence of higher amount of Ca compared to K within vermiculite flakes (Table 3) indicating removal of alkalis during the supergene process.

9. CONCLUSIONS

The formation of Agasthyapura vermiculite deposit is similar to those reported for several vermiculite deposits elsewhere - vermiculite bodies

found along ultramafic rock-felsic intrusive contacts - such as examples in Egypt (El Shazly et al., 1975), and in Wyoming and North Carolina in the U.S.A. (Hagner, 1944; Kulp and Brobst, 1954). Field, textural and physico-chemical characteristics of vermiculite from Agasthyapura area indicate locally complete alteration of ultramafic rock bodies due to the fluid reactions during acidic intrusion. The process of alteration is mainly due to saline aqueous fluids which accompanied the acidic intrusions. This hypogene process formed secondary phases, such as hornblende and biotite. The alteration of biotite to vermiculite through an intermediate stage of hydrobiotite is interpreted as a supergene event caused by the circulation of ground water, which leached potassium from biotite and then from hydrobiotite, ultimately forming vermiculite.

ACKNOWLEDGEMENTS

The authors are grateful to USGS for SEM and microprobe data. We thank Prof. C. Srikantappa, Chairman, Dept. of Geology, Univ. of Mysore, India, for constant encouragement and help.

REFERENCES

- Bassett, W.A.: 1959, The origin of the vermiculite deposit at Libby, Montana, *American Mineralogist*, 44, No. 3 & 4, 282-299.
- Boettcher, A.L.: 1966, Vermiculite, hydrobiotite, and biotite in the Rainy Creek igneous complex near Libby, Montana. *Clay Minerals*, 6, 283-296.
- Bush, A.L.: 1976, Vermiculite in the United States, in Eleventh Industrial Minerals Forum, Montana Bureau of Mines and Geology, Special Publication 74, 145-155.
- Cariati, F., Erre, L., Micera, G., Piu, P., and Gessa, C.: 1983, Effects of layer charge on the near-infrared spectra of water molecules in smectites and vermiculites, *Clays and Clay Minerals*, 31, No. 6, 447-449.
- Chattopadhyay, G. and Bhattacharyay, A.K.: 1994, Vermiculite mineralization in parts of Palamau district, Bihar. *Indian Journal of Earth Sciences*, 21, No. 3, 148-152.
- de la Calle, C. and Suquet, H.: 1988, Vermiculite. In *Hydrous Phyllosilicates (Exclusive of Micas)*, S.W. Bailey, ed., Mineralogical Society of America, Washington, D.C., 455-496.
- El Shazly, E.M., El Ramly, M.F., Saleeb Roufaiel, G.S. and Rasmy, A.H.: 1975, Geology, petrogenesis and mode of formation of asbestos-vermiculite deposits of Hafafit, Egypt. *Egyptian Journal of Geology*, 19, No. 2, 87-104.
- Fatma Toksoy-Koksal, Asuman, G. Turkmenoglu and Cemal Goncuoglu M.: 2001, Vermiculitization of Phlogopite in metagabbro, Central Turkey, *Clays and Clay Minerals*, 49, No.1, 81-91.
- Ghabru, S.K., Mermut, A.R., and St. Arnaud, R.J.: 1987, The nature of weathered biotite in sand-sized fractions of gray luvisols (boralfs) in Saskatchewan, Canada. *Geoderma*, 40, 65-82.
- Gruner, J.W.: 1934, Structures of Vermiculite and their collapse by dehydration, *American Mineralogist*, 19, 557-575.
- Hagner, A.F.: 1944, Wyoming vermiculite deposits, *Geological Survey of Wyoming Bulletin*, 34, 26-28.
- Jelitto, J., Dubinska, E., Wiewiora, A. and Bylina, P.: 1993, Layer silicates from serpentinite-pegmatite contact (wiry, Lower Silesia, Poland), *Clays and Clay Minerals*, 41, 693-701.
- Komarneni, S. and Roy, R.: 1981, Hydrothermal transformations in candidate overpack materials and their effects on cesium and strontium sorption, *Nuclear Technology*, 54, 118-122.
- Kulp, J.L. and Brobst, D.A.: 1954, Notes on the dunite and the geochemistry of vermiculite at the Day Book dunite deposit, Yancey County, North Carolina, *Economic Geology*, 49, 211-220.
- Lemlein, C.C and Klevstov, P.V.: 1961, Relations among the principal thermodynamic parameters in a part of the system H₂O-NaCl, *Geochemistry*, 2, 148-158.
- Melka, K.: 2000, Transitional phases of mica crystals in volcanic materials, *First Latin-American Clay Conference, Funchal - Madeira, Vol. 1*, 306-316.
- Melka, K., Adamová, M. and Haladová I.: 2000, Mixed-layer crystal structures of the hydrobiotite type in tuffs of the Doupovské hory Mts. region, *Scripta Fac. Sci. Nat. Univ. Masaryk. Brun.*, 28-29, *Geology, Brno*, 7-18.
- Melka, K., Ulrych, J. and Mikuláš, R.: 2005, Hydrobiotite from the Dětaň oligocene tuffs (Doupovské hory Mts.), *Acta Geodyn. Geomat.*, Vol. 2 (138), 119-129.
- Moore, D.M. and Reynolds, R.C., Jr.: 1989, *X-ray Diffraction and Identification and Analysis of Clay Minerals*. Oxford University Press. Oxford, pp. 332.
- Morel, S.W.: 1955, Biotite in the basement complex of Southern Nyasaland, *Geological Magazine*, 92, 241-255.
- Nemecz, E.: 1981, *Clay Minerals*. Akademiai Kiado, Budapest, Hungary, 547.
- Nakamuta, Yoshihiro: 1981, A regularly interstratified chlorite/vermiculite in a talc-chlorite vein, *Memoirs of the Faculty of Science, Kyushu University, Series D: Geology*, 24, No. 4, 253-279.
- Nettleton, W.D., Nelson, R.E., and Flach, K.W.: 1973, Formation of mica in surface horizons of dryland soils, *Soil Science Society of America Proceedings*, 37, No. 3, 473-478.
- Prakash Narasimha, K.N., Bradley Van Gosen, Heather A. Lowers, P.S.R Prasad, Krishnaveni and Ramalingaiah: 2004, Vermiculite Mineralization in Gopalapura Area, Mysore District, Karnataka, Abstracts: VI Convention of

- Mineralogical Society of India and International Seminar on Earth Resources Management, 28-30th January, Kuvempu University, Shankarghatta, Shimoga, Karnataka, 16.
- Prakash Narasimha, K.N, Krishnaveni, Prasad, P.S.R, Ramalingaiah, H. and Venugopal, J.S.: 2006, Vermiculite in the Gopalpura area, Karnataka - A mineralogical study, Jour. Geol. Soc. Ind., 67, No. 2, 159-163.
- Prasad, U. and Majumdar, M.K.: 1966, A note on the hydro-biotites of Bhagalpur and Santhal Parganas districts, Bihar, Indian Minerals, 20, No. 1, 45-48.
- Radhakrishna, B.P.: 1948, Vermiculite in Mysore - Bangalore, India, Current Science, 17, 212.
- Radhakrishna, B.P. and Vaidyanadhan, R.: 1997, Geology of Karnataka, Geological Society of India Publication, pp. 353.
- Roy, R and Romo, L.A: 1957, Weathering studies: I New data on Vermiculite, Geology Journal, 65, 603-610.
- Ruiz Cruz, M.D.: 2003, Two stages of "metamorphic vermiculite" growth in schists from the Malaguide Complex, Betic cordillera, Spain, The Canadian Mineralogist, 41, No. 6, 1397-1412.
- Ruiz Cruz, M.D. and Novák, J.K.: 2003, Metamorphic chlorite and "vermiculitic" phases in mafic dikes from the Malaguide Complex (Betic Cordillera, Spain), European Journal of Mineralogy, 15, No. 1, 67-80.
- Sourirajan, S. and Kennedy, G.C.: 1962, The system H₂O-NaCl at elevated temperature and pressure, Am. J. Sci., 260, 115-141.
- Swaminath, J and Ramakrishna, M.: 1981, Early Precambrian Supracrustals of Southern Karnataka, Memoirs of the Geological Survey of India, 112.
- Tarzi, J.G., and Protz, R.: 1979, Increased selectivity of naturally weathered biotites for potassium, Soil Science Society of America Journal, 43, No. 1, 188-191.
- Van Gosen, B.S., Lowers, H.A., Bush, A.L., Meeker, G.P., Plumlee, G.S., Brownfield, I.K. and Sutley, S.J.: 2002, Reconnaissance study of the geology of U.S. vermiculite deposits - Are asbestos minerals common constituents?, U.S. Geological Survey Bulletin 2192, 8.
- Zhelyaskova-Panayotova, M., Laskou, M., Economou, M. and Stefanov, D.: 1992, Vermiculite occurrences from the Vavdos and Gerakini Areas of the W.Chalkidiki peninsula, Greece, Chemical Erde, 52, 41-48.
- Zhelyaskova-Panayotova, M., Economou- Eliopoulos, M., Petrov, P.M., Laskou, M. and Alexandrova, A.: 1993, Vermiculite deposits in the Balkan peninsula, Bulletin of Geological Society of Greece, 28, 451-461.



Fig. 2 Vermiculite mineralization trending in N70°E-S70°W direction at the contact of acid intrusive and ultramafic rock.



Fig. 3 Alteration of clinopyroxene to biotite and to vermiculite along grain boundaries (under polarizing microscope).



Fig. 4 Alteration of hornblende along grain boundaries to vermiculite (under X nicols).

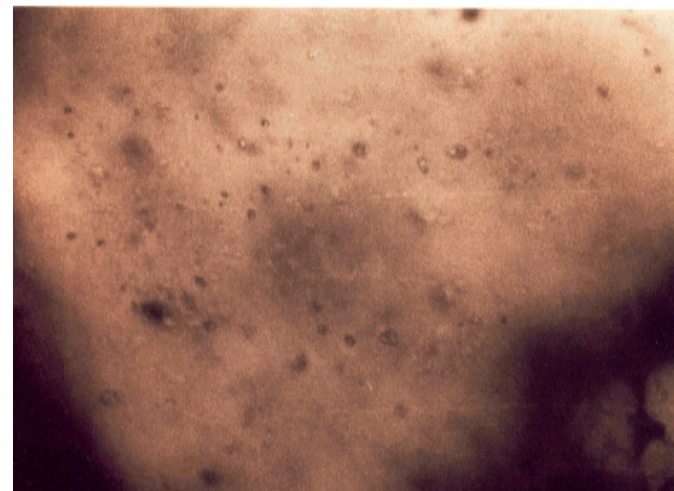


Fig. 7a Randomly distributed aqueous inclusions in quartz grain.